A Flexible, Multi-fidelity Levelised Cost of Energy Model for Floating Offshore Wind Turbines Multidisciplinary Design, Analysis and Optimisation Approaches

V Sykes[1,*], M Collu[1] and A Coraddu[2]

[a]The department of Naval Architecture, Ocean and Marine Engineering, The University of Strathclyde, Glasgow G4 0LZ, UK
[b]The Department of Maritime Trasport Technology, Delft University of Technology, 2628 CD Delft, The Netherland

*Corresponding author: victoria.sykes@strath.ac.uk

Abstract. As the UK takes a step towards a greener, cleaner future aiming to be net zero by 2050, continuous development of the power network is required. A clear solution is offshore wind, having already proved its feasibility and success in nearshore sites. However, a large majority of near shore sites in the UK are already being utilised. The next step is to move into deeper waters and utilise the stronger, more consistent wind resources. A solution could be floating offshore wind which is still in its infancy, with only a few operational floating wind farms installed. Building upon the multidisciplinary design, analysis, and optimisation framework (MDAO) for floating offshore wind turbines (FOWT) being developed at the University of Strathclyde, called FEDORA, the aim of this work is to refine the LCoE model adopted by FEDORA, and applying it to perform the optimisation of the floating offshore OC3 SPAR. There is limited data on cost, therefore Hywind Scotland Pilot Park will be used as a basis for the LCoE model, allowing the results to be validated. This model is not restricted to SPARs, as it establishes a general methodology to calculate the life cycle cost of floating offshore wind farms. Utilising the improved cost model this work finds four optimised SPAR structures for four different maximum angles of inclination which can be experienced in the wind turbines operation. The improved cost model has a much higher accuracy, highlighting the initial cost model underestimates the cost of the SPAR structure by around half.

1. Introduction

Wind turbines have been proven effective both onshore and fixed offshore, producing a green energy capacity of 12 GW onshore and 10.5 GW offshore in the UK alone [1]. Due to the geographical characteristics of the UK, it has a prime resource to be exploited, making the UK the world leader in offshore wind with the largest installation around the globe. With a large quantity of fixed offshore turbines currently installed, the UK Government has pledged to power all homes through green wind energy by 2030, requiring the current capacity to increase fourfold. Scotland is aiming to be net zero by 2045, and the UK by 2050. A steppingstone in this colossal change will be increasing wind power: it is estimated by Statoil that 80% of Scotland's wind resource is in waters deeper than 60m, making the case to go further offshore stronger than ever [2].

In order to meet this rapid increase in capacity, wind resources further offshore will have to be utilised. However, conventional fixed-to-seabed support structures are no longer viable in terms of cost and inherent difficulties to design and install them [3]. This is pushing the industry to evolve and implement floating support structures. The floating typology offers a host of advantages such as: flexibility in construction and installation, reduction in sensitivity to water depth, resistance to higher wind speeds, reduced vessel costs, reduced damage to seabed, and potentially lower decommissioning costs [4]. Moving offshore does, however, have inherent issues, such as higher failure rates, lower reliability, and higher O&M costs [5].

Since there have only been a few prototypes installed, and the first FOWFs have only been operating for a few years, there is limited information on the LCoE: current findings have estimated LCoE ranging between 67 and 287.8€/MWh [6], much higher than fixed bottom wind turbines.

A substantial amount of research has been previously conducted on LCoE of offshore wind farms in shallow waters (fixed turbines), but the literature on FOWF LCoE is still relatively scarce. The aim of this work is to create an adaptable model for LCoE which can be implemented in any MDAO framework for floating wind farms. The implementation of a multi-fidelity approach will make this model more applicable to a range of MDAO approaches, ensuring that even with a minimal amount of data, as often is the case in early design phases, a cost can be estimated. Within the MDAO framework FEDORA, the cost related to the SPAR support structure needs to be calculated at each step of the optimisation, i.e. for each configuration proposed, and this can be considered as a constraint or an objective of the optimisation. As a case study, this research will focus primarily on a location off the coast of the Shetlands, Scotland, in the North Sea region. This area sees mean wind speed greater than 9m/s, making it a prime location for wind farms [7]. The Hywind site has been selected as a case study due to the abundance of data available, facilitating the verification/validation of the model here developed. The NREL 5MW turbine will be utilised for this case study, as there is already information for it within the FEDORA model and data are readily available in publicly available sources.

The work conducted in this paper is arranged as follows: - section 1 provides a general overview of the paper and topic area, section 2 gives an overview of the existing literature and the aims and objectives of this paper, section 3 presents the methodology to obtain the optimised OC3 SPAR, with its cost as an objective, comparing the results to the literature ensuring validation, and in section 4, a case study of the full LCoE of the selected site is presented, again comparing calculated data to the literature. Finally, section 5 offers the main finds of the report and draws a conclusion.

2. Related Work

Due to the exposure to the harsh environment, stronger winds, and the potential for larger turbines, the capital cost of FOWTs is predicted to be doubled in comparison to fixed platforms [7], [8]. It is also expected that Operations and Maintenance (O&M) costs would increase due to increased journey times, harsher environments, more expensive vessels, and reduced weather windows [11], [12]. The increase in cost in comparison to fixed bottom turbines is hoped to be counteracted by a higher and more consistent energy yield, allowing the FOWT's to achieve competitive LCoE [5], [6], [11].

Various research has been carried out with varying levels of detail to determine the cost of floating SPARs for wind turbines [6], [8], [12]–[17]. Table 1 highlights the data found within the literature. This can be used as a guide to validate the model.

Table 1. CAPEX, OPEX, DECEX and LCoE found in the literature for floating offshore SPARs.

Reference	[17]	[13]	[6]	[8]	[12]	[14]	[18]	[19]	[20]	[11]
CAPEX (£M/MW)	1.6	2.3-3.1	3.1	2.5	2.1	3.1	4.57	1.8	-	2.1
OPEX (£M/MW)	-	0.75	0.5	0.67	0.9	0.6	0.63	0.70	-	1.1
DECEX (£M/MW)	-	-	0.5	0.7	$1.2e^{-3}$	-	-	0.2	-	0.1
LCOE (£/MWh)		117.4-120	70.3-92.6	80.7	-	138	113.1	93-142.4	158.5	-

Research by C. Maienza, et al. [8] covers the three main types of FOWT sub-structures, finding cost data for CAPital EXpenditure (CAPEX), OPerational Expenditure (OPEX) and DECommissioning EXpenditure (DECEX), using a linear regression to calculate each cost parameter. The installation calculation considers six different techniques to install the turbine, allowing the cost estimation to be more accurate. The O&M model uses the probability of a failure to occur for different components, determining both corrective and preventative maintenance costs. Similar methods for O&M calculation were used in S. Alsubal, et al., [19].

Anders et al., [21] carries out a cost comparison for the six main floating concepts. This paper has detailed information of the time and cost for installation of different components, vessel hires, and technicians required. The research deduces that the LCoE of floating offshore is not vastly greater than that of fixed wind turbines.

Alsubal et al., [19] has an in depth explanation of formulations used to find cost data for floating offshore wind, while also utilising the Weibull Probability Density Function (PDF) to determine the Annual Energy Production. Contributions in terms of percentage of total cost are presented alongside the $/MW for each individual cost element.

Similarly, for the North of Spain and Portugal, Castro-Santos et al. [20], [11] created a cost model which considers bathymetry, wave data and distance to port. This model looks at a large area of sea for each country where the resource has high potential, calculating the LCoE for the full area, allowing both the area of lowest LCoE and appropriate substructure to be pinpointed.

Cost models have been used repeatedly within optimization frameworks with one of the main objectives being to minimise cost. However, the cost models utilised are more often than not a poor representation of cost, generally based on a £/kg value [22]–[30]. Another method used to consider the cost is reducing the mass of the structure, which is related to cost, however, this is, again, relatively poor [31]–[36]. Improved models by Hegseth et al. [37] include the £/kg of the structure and the fabrication cost related to time to carry out the work. Optimization of a OC3 SPAR and Hexafloat support structure was carried out in [13] also utilising a £/kg value within the cost model. In this work a higher steel density is considered in-order to account for welding and flanges which would otherwise be neglected. Zhou et al. [30] constrains semi-submersibles geometry variables in order to optimize the structure with the hope to reduce the cost. The cost model used for the semi-submersible in their research includes the manufacturing costs: Material cost, labour costs, welding and painting. This paper provides a more accurate cost for the support structure but does not include cost as a constraint within the optimization.

A gap highlighted in the literature is the need for a more accurate cost model which can be used within the optimization itself. The aim of this work is to create two cost models for the structural cost of the SPAR, one being a £/kg model and the latter being a more accurate model, giving the user more flexibility particularly when in early design stages. These models can then be used in the optimisation of the SPAR shape for a range of maximum inclination angles. The structural cost can then be plugged into the LCoE model for any given site.

3. Methodology

Firstly, a few assumptions were made within the cost model. The layout of the offshore wind farm was based on the radial formation as this is most used within industry. This layout ensures that the wind turbines are four diameters apart inter-row and seven diameters apart in-row [20]. For simplicity within the cost model, the distance to shore was used when determining vessel hire and other related costs, whereas in real life scenarios, it would be distance to port, requiring all ports surrounding the area to be mapped out in order to determine which is closest and has the capability to handle the support structure. A limitation of the cost model is the exclusion of losses. Currently only the electrical cable losses are considered.

The methodology of this research is depicted in Figure 1, highlighting the optimization process and the range of fidelities within the model. The initial stages involve data acquisition for the cost model. The input data for the selected site, Hywind, and cost data related to offshore floating wind turbines was

found within literature [38], [39]. Using the combination of cost, wind turbine and site data, the cost model was created with the total cost split into CAPEX, OPEX and DECEX.

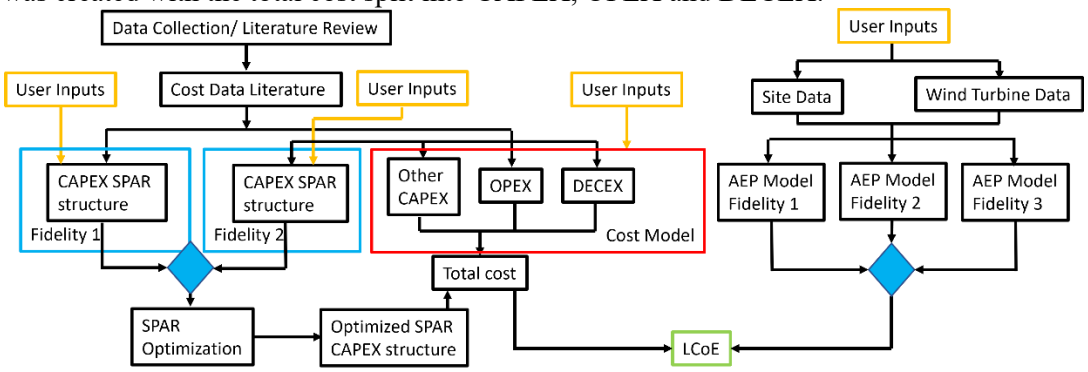

Figure 1. Methodology Flow Chart

The cost model implements a multi-fidelity approach and focuses on the floating wind turbine substructure costs. The lower level of fidelity (fidelity 1) for the substructure cost has one input, steel mass of the structure. This reduced cost model focuses purely on finding a benchmark value for the OC3 SPAR. The FEDORA model utilises twelve truncated cones for the SPAR hull, the higher level of fidelity (fidelity 2) includes this notion by calculating the volume of the hollowed cones, which can be used to find the total cost of not only mass but other related manufacturing costs.

Estimating the dynamic response at a given sea state is critical in ensuring the platform is obtaining the desired performance. In the FEDORA model, the dynamic response analysis is carried out in the frequency domain and is described by the Response Amplitude Operator (RAO). To carry out this analysis, the centre of gravity, mass matrix, centre of buoyancy, hydrostatic, and wave loads are required. The first step to find centre of gravity and the mass matrix is defining the geometry. To do this for the given optimisation problem, parametrization of the geometry is necessary. Rather than being confined to a singular cylinder to represent the SPAR, FEDORA utilises a number of truncated cones allowing a greater set of geometries to be explored, potentially leading to a novel, more cost-effective solution. The geometry can be expressed as:

$$[c, r_0, R1, \dots, r_c, T]$$

Where c is the number of cones, r_0 is the upper radius and T is the draft of the SPAR. When determining the mass distribution, the rotor-nacelle assembly and tower mass moments of inertia and centres of gravity, $M_{3,3}^{WT}$ and z_G^{WT} respectively, have been considered constant for all analysis carried out. Similarly, the mooring system is also considered constant and is expressed as a stiffness matrix when finding the RAOs. Hence the mass, moment of inertia, and CoG of the floating support structure is dependent on the design vector presented above. The mass is then presented as the sum of the structural mass, $M^{SD} \in \mathbb{R}^{6\times6}$, and ballast material, $M^{SB} \in \mathbb{R}^{6\times6}$, with corresponding CoG respectively given as $z_G{}^{SD} \in \mathbb{R}$ and $z_G{}^{SB} \in \mathbb{R}$. The total mass matrix, M, and centre of gravity, z_G, are represented as follows, where $_{3,3}$ represents heave direction:

$$M = M^{WT} + M^{SD} + M^{SB}$$

$$z_G = \frac{1}{M_{3,3}}\left(z_G^{WT} M_{3,3}^{WT} + z_G^{SD} M_{3,3}^{SD} + z_G^{SB} M_{3,3}^{SB}\right)$$

To find the hydrodynamic characteristics of the platform, the total restoring matrix, $C \in \mathbb{R}^{6\times6}$, added mass matrix, $A \in \mathbb{R}^{6\times6}$, radiation damping matrix, $B \in \mathbb{R}^{6\times6}$, and first order wave load transfer function, $X \in \mathbb{R}^{6\times1}$, are required. From the geometry vector, the CoB can be found as the weighted centre of volume for each truncated cone. Since the geometry is asymmetrical around the vertical axis, the longitudinal and lateral position of the CoB is zero. With this information, the total hydrostatic and gravitational restoring matrices ($C^H \in \mathbb{R}^{6\times6}$ and $C^G \in \mathbb{R}^{6\times6}$) can be derived according to [40], including the mooring stiffness, the total stiffness matrix, C is the summation of the three. The calculation of A, B, and X are significantly more complicated and demanding to find. It is for this reason Boundary

Element Method (BEM) is used to solve partial differential equations which are encountered in the radiation and diffraction potential flow problems. This work utilses the software NEMOH to find A and B, giving both as a function of wave frequency, ω. The wave loading is, however, presented as a function of frequency and wave direction. For simplicity, coupling effects have been neglected from this work and only surge, heave and pitch are calculated. The six motions of a floating body in regular waves can be expressed as follows:

$$\sum_{j=1}^{6} \xi_j \left[-\omega^2\left(M_{i,j} + A_{i,j}\right) + i\omega B_{i,j} + C_{i,j}\right] = \eta X_i \qquad i \in \{1, \dots, 6\}$$

Where ξ_j is the j-th degree of freedom displacement and η is the wave amplitude. Rearranging this equation, it can be solved to find the body's displacement in the j-th degrees of freedom. The complex response transfer function between the wave amplitude and the oscillatory amplitude is then:

$$H_j = \frac{\xi_j}{\eta} = \sum_{j=1}^{6} \left[-\omega^2\left(M_{i,j} + A_{i,j}\right) + i\omega B_{i,j} + C_{i,j}\right]$$

Since the RAO is a function of wave frequency, comprised of both magnitude and phase, the RAO magnitude in the given degree of freedom, is defined as the complex magnitude of the transfer function H_j.

The optimisation problem has been implemented considering a single objective function, and four main constraints. The objective function to be minimised, focuses on the minimisation of the LCOE, approximated (due to the early design phase at which this optimisation takes place) as explained in the relevant sections.

In terms of main constraints, the following have been considered:

- floatability
- max nacelle acceleration
- max total pitch angle of inclination
- positive static stability

Floatability is ensured by verifying that the total weight force of the whole system (including the Rotor-Nacelle Assembly, the tower, the floating substructure, and the ballast mass), plus the downward vertical component of the total mooring tension, is equal to the total buoyancy force. Numerically, this is ensured by deriving the ballast mass necessary, and ensuring that this is a positive number.

In terms of max nacelle acceleration, this refers to the fact that some of the equipment and mechanical components inside the nacelle may be exposed to abnormal inertial loads when the acceleration at nacelle level exceed a certain limit, and therefore a max acceleration at nacelle level is imposed. Numerically, since the present work is based on a frequency domain approach, the acceleration at nacelle level has been calculated by deriving the fore-aft nacelle acceleration response amplitude operator, function of the surge and the pitch response amplitude operators, and coupling it with the specified wave spectrum, to derive the fore-aft nacelle acceleration response spectrum, and from this the significant amplitude of this acceleration. Quantitatively, the significant amplitude of this acceleration has been limited to a max value equal to 6 m/s^2, i.e. 0.6g.

The overall system pitch angle, i.e. the total angle of inclination of the overall floating wind turbine system, has been limited to 10 deg. This angle is the sum of an average (static) component, due to the inclining moment, originating from the aerodynamic thrust acting on the rotor and the counteracting horizontal component of the mooring restoring force, and an oscillatory component, due to the (first order) wave loads acting on the floating substructure. For the oscillatory component, the significant amplitude of the oscillation, calculated with the pitch displacement response amplitude operator and the wave specturm, has been added to the static pitch angle component, to calculate the total pitch angle.

The last constraint is necessary from a mathematical point of view, since a "negative" static stability, i.e. an unstable system from a static stability point of view, would satisfy at mathematical level the above constraints, but would represent an unphysical solution - therefore the total stiffness coefficient in pitch

has been constrained to positive values. The total stiffness coefficient in pitch includes the contribution from the gravitational stiffness, the hydrostatic stiffness, and the (limited, since a catenary mooring system is considered) stiffness in pitch provided by the mooring system, calculated as shown by Collu in [41].

The optimization itself is carried out considering a JONSWAP spectrum with a significant wave height of 10m and peak period of 18.5 seconds. NEMOH is used, in order to compute first order wave loads on the offshore structure. This is carried out for a frequency range 0.05rad/s to 1.25rad/s with 0.05 increments. To find a realistic SPAR shape, the radius was constrained to be between 0.5m and 7.5m and the draft of the whole axisymmetric support platform was constrained to be between 100m and 140m. The optimisation needs a starting point and was given a radius 3.5m and a height of 120m, the closest to the Hywind Scotland Pilot Park SPAR configuration.

The other costs, at this level of approximation are not related to the SPAR dimensions, hence these can be calculated after the optimisation has been done, reducing computational time. The total cost can then be found, with a breakdown as follows: concept definition, design and development, manufacturing, installation, Operation and Maintenance (O&M), and decommissioning.

As previously expressed, there are four main categories of CAPEX, and the model calculates them as follows. Concept definition cost [12]:

$$C1 = (C_{legal} + C_{survey} + C_{contingency})P_{WF}$$

This determines the cost to carry out surveys, legal, and contingencies fees of the offshore wind farm. These costs are expressed in £/MW therefore have to be multiplied by the wind farm's total power, P_{WF}. Design and engineering cost [12]:

$$C2 = (C_{Projm} + C_{Eng})P_{WF}$$

Where C_{Projm} is project management costs and C_{Eng} is engineering costs per MW. The manufacturing cost is divided into tower, substructure, mooring and anchorage, nacelle, blades, monitoring, and electrical system. The Tower cost can be found as $C31 = m_t C_m$, where C_m is the material cost and m_t is the mass of the tower. The density of steel considered for the tower is 8500kg/m^3 this allows paint, bolts, welds and flanges to be accounted for [38]. The manufacturing costs of the substructure has two levels of fidelity. The first is based on £/kg as follows: $C32 = m_p C_m$, where m_p is mass of the platform. Fidelity level two support structure cost is split into five subcategories: material cost, forming, axial butt welds, circumferential welds, and paint. The formulations for these calculations can be found in [42].

The nacelle (C33), blades (C34) and monitoring (C37) are based upon a £/MW calculation. Mooring and anchorage costs (C35) can be found using, $C35 = C_{chain}L_{chain} + C_{anchor}No_{anchors}$.

C_{chain} and C_{anchor} is the cost of the chain (per meter) and anchor respectively. L_{chain}, is the total length of chain required for all wind turbines and $No._{Anchors}$, is the total number of anchors required for the wind turbine. Finally, the electrical system cost (C36) is comprised of the following [12]:

$$C36 = CPlat_{onshore} + CPlat_{offshore} + C_{export}L_{export} + C_{array}L_{array} \ldots + C_{cablelosses}L_{export}P_{WF}$$

Including fixed costs for onshore and offshore platforms, the cost of array and export cables considering the length of each, and the cost related to cable losses. Total manufacturing cost is found as:

$$C3 = C31 + C32 + C33 + C34 + C35 + C36 + C37$$

Installation costs are split into port, cable, substation, anchor and mooring, platform, and turbine. The port formula for cost is as follows:

$$C41 = \left(No_{cranelifts} + C_{Tech}NO_{tech}\right)T_l \times NO._{Turb}$$

Using the number of lifts carried out per turbine, $No_{cranelifts}$, the number of turbines, $NO._{Turb}$, crane hire cost and the hourly rate of a technician, C_{Tech}, the number of technicians, NO_{tech} all multiplied by the number of hours to carry out a lift, T_l.

A generic formula can be written for the other installation costs consisting of crew, fuel and vessel hire costs [8], [43]:

$$C_{Fuel} = C_f \times F_r \left[T_i + \left(\frac{2 \times D}{V_s}\right)\right]$$

$$C_{vessel\ hire} = C_V \left[T_i + \left(\frac{2 \times D}{V_s}\right)\right]$$

$$C_{crew} = C_{Tech} \times NO_{tech} \left[T_i + \left(\frac{2 \times D}{V_s}\right)\right]$$

Where, C_f, is fuel cost, F_r, is fuel consumption, T_i, is time to install the turbine, D is distance to shore, V_s, is vessel speed and, C_V, Vessel hire rate. Different vessels were required for each installation task. Total installation cost (C4)[8], [43]:

$$C4 = C41 + C42 + C43 + C44 + C45 + C46$$

The OPEX (C5) and DECEX (C6) costs are calculated using a £/MW estimate costs [8], [19]:

$$C5 = (C_{Indirect} + C_{direct})P_{WF} + C_{insurance}(C1 + C2 + C3 + C4)$$

$$C6 = (C_{Decom} + C_{siteclear})P_{WF}$$

$C_{Indirect}$, are indirect maintenance costs such as vessel hire and coordination of providing a repair service. C_{direct}, are directly related costs to replace the failed components and technicians. This category can also be further divided into preventative and corrective maintenance. $C_{insurance}$, is the cost of insurance and is a percentage typically taken as 1% of the total CAPEX [44].

C_{Decom}, is the cost to decommission the site, i.e., to remove the wind turbines and their support structures. $C_{siteclear}$, is the cost to clear the site to ensure it is in accordance with regulations. The total cost of the FOWF can be found by summing C1 to C6.

In order to find the LCoE of the farm, the Annual Energy Production (AEP) was also found. Three levels of fidelity have also been implemented for AEP calculation. The first is a simpler model only utilising a single value for each Weibull parameter, whereas the latter model uses 12 values for each parameter allowing seasonal variation to be accounted for [39]. The third level of fidelity exploits a time series. The Weibull parameters were then fit to this data in order to get the probability density function.

To calculate the AEP, the probability of each wind speed occurring for the given site must be estimated. The first two fidelity model for AEP require different inputs. Using this information, the wind speed, U_n, can be found at the hub height (87.6m) using the log law. The roughness, z_o for the site needs to be considered and can be found using the two wind speeds at the two different heights, z_n with the same logarithmic rule. For the Hywind site wind speed data for 10m and 100m were used. Finally, both location and shape parameters do not change with height, however, the scale parameter changes linearly with height. The Weibull PDF function could then be plotted using its formula. In order to obtain AEP, it must be combined with the power curve of the 5MW NREL wind turbine, see Figure 2.

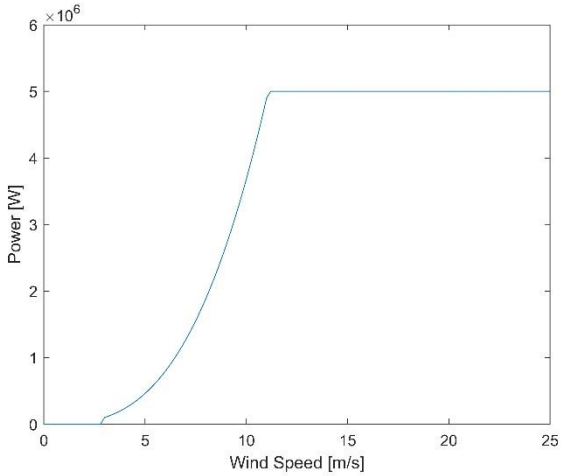

Figure 2. NREL 5MW wind turbine power curve

The LCoE can then finally be calculated using formula below, where r represents the discount rate and n is the number of operational years:

$$LCoE = \frac{\frac{Total\ cost}{(1+r)^n}}{\frac{AEP}{(1+r)^n}}$$

4. Results and Discussion

A general optimisation problem is defined as either a maximisation or minimisation of a specific objective function which is subjected to constraints and a set of design variables. The optimisation problem presented in this work has one objective which is to reduce cost while maintaining acceptable hydrodynamic performance. The analysis was carried out in MATLAB using the Pattern search optimisation algorithm.

The optimisations were run for four different maximum angles of inclination 5°, 7°, 7.5° and 10° all yielding slightly different shapes, see Figure 3. The purpose of varying the maximum angle of inclination is namely to gain an understanding of constraint relaxation and its benefits, and to capture a range of operational conditions the SPAR could potentially operate under.

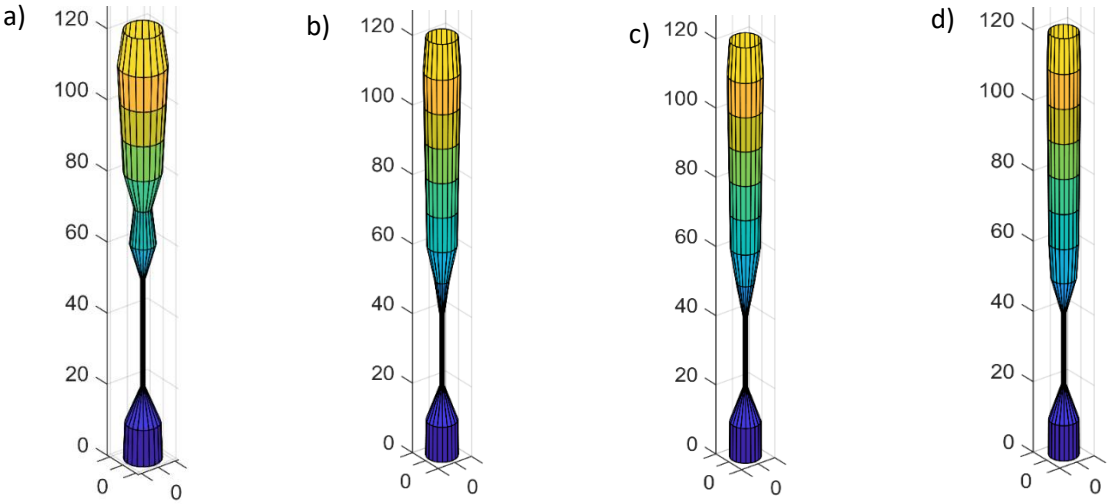

Figure 3. Optimised SPAR shapes a) 5° angle of inclination, b) 7° angle of inclincation, c) 7.5° angle of inclincation and d) 10° angle of inclincation.

The optimization was run for both cost models yielding the same optimized shape, but inherently different costs were calculated, see Table 2.

Table 2. Cost calculated for each angle of inclination.

Angle of Inclination (°)	5	7	7.5	10
Model 1	£1,716,000	£1,363,000	£1,320,000	£1,180,000
Model 2	£3,705,000	£2,916,000	£2,822,000	£2,522,000

As the angle of inclination is increased a pattern of decreasing radii is noticed, along with a decrease in cost. It makes sense for both parameters to decrease together as they are heavily linked. They are expected to decrease with increasing inclination due to the static stability of the SPAR. The main contributor to static stability is the vertical distance between the center of buoyancy (CoB) and center of gravity (CoG). By constraining the maximum allowable angle of inclination, a larger distance between CoB and CoG is required. The optimiser obtains this larger distance by increasing the radius of the upper section of the SPAR 'pushing' the CoB upwards, creating a 'champagne flute' shape.

It is clear from Table 2, that there is a noticeable difference in the cost model values with the biggest difference seen for 5° angle of inclination, with an increase of around 215%. This highlights the issue of assuming a £/kg value for the structure.

A key comparison is the cost of the non-optimised SPAR and the optimised SPAR. For cost model one the unoptimized SPAR is £1.33 million and £2.83 million for cost model 2. The non-optimised case considers no inclination, being a potential reason why the 5° of inclination models have a higher value for the optimised case, along with the fact that the SPAR for 5° has a larger radius over the depth of the platform compared to the other platforms for different inclinations. Overall, for all other angles of inclination other than 5° and 7° for the second cost model, the cost is reduced compared to the un-optimized case. At the Hywind site the OC3 Spar-buoy platform is utilised, which has an inclination angle of 7.5°. Comparing the results calculated for this angle it can clearly be seen that the optimisation produces a lower cost.

Table 3 shows a lack of consensus on how much the support structure would cost ranging from £2.27 million to £9.4 million for the SPAR. This comes from varying detail in cost models and assumptions made by different authors. All values calculated for the SPAR buoy fall within this range, being closest to work done in [14] and [21].

Table 3. Cost literature for support structures.

Reference	CAPEX of SPAR	units	£M (5MW)	SPAR Type	Absolute error	Absolute relative error
[13]	7.5	£M	7.50	OC3 SPAR	4.68	62.40%
[14]	0.454143	£M/MW	2.27	Generic	0.549285	24.19%
[8]	136.9	€M (125MW)	4.65	OC3 SPAR	1.8346	39.41%
[12]	235.8	€M(106.575W)	9.40	Generic	6.583237	70.01%
[21]	3.47	€M(5MW)	2.90	OC3 SPAR	0.08	2.76%
Model 2 (7.5°)	2.82	£M(5MW)	2.82	OC3 SPAR	-	-

5. Case Study

The case study, which implements 5 x 5MW NREL turbines at an inclination of 7.5° located on the Hywind site, compared to the 6MW turbines used at the site currently, finds the higher fidelity model calculating an LCoE of £116.47/MW, and comparing this against data in the literature, the approach is verified [11], [12], [20]. The full cost breakdown can be seen in Table 4.

The lower level of fidelity model finds an LCoE of £104.46/MW again falling in line with estimates within research [11], [12], [20], [21]. The AEP level three fidelity approach estimates a total energy of 1.2957×10^{11}Wh, while the lower fidelity one a value of 1.112×10^{11}Wh. The highest fidelity model requires a time series of data and 7 parameters related to wind turbine as input data, compared to 12 parameters, without any times series, for the lower fidelity one, however, the AEP highlights that there is a trade off in terms of accuracy vs simplicity and time with a slight underestimation with the reduced model. Nonetheless, this can be considered a good starting point as the output is relatively similar. Adding a range of fidelity to both the cost and AEP models, creates a more flexible model, allowing cost to be calculated with a limited amount of knowledge of the site and wind turbine. This flexibility makes it much easier to implement in other MDAO frameworks, no matter how detailed or vague they are. To find the LCoE for this paper fidelity three was used.

When calculating the cost of the floating offshore SPAR, a key take-away is that not all costs are related to the SPAR sub-structure specific geometry itself. Inherently, the cost of manufacturing, installing, O&M related to the SPAR, and station keeping system selected are heavily dependent on the support structure typology itself (SPAR). The decommissioning and operation and maintenance costs also depend on the typology of the support structure, as this will influence the vessel required to remove it and failure rates of the structure. Several of the approaches adopted to quantify the costs considered in the present paper are also applicable to both Semi-submersibles and Tension Leg Platforms and could be used within a model for such platforms. These costs are concept, design and engineering costs, and the manufacturing and installation of the wind turbine and electrical system [8].

Table 4. Cost Breakdown of the floating offshore wind farm.

			Model 1	Model 2	Model 1	Model 2	[19]
CAPEX	Concept	C1	£5.25M		8%	7%	77%
	Design and Engineering	C2	£1.68M		2%	2%	
	Manufacturing	C3	£31.74	£39.25M	47%	52%	
	Installation	C4	£10.71M		16%	14%	
OPEX	Operation & Maintenance	C5	£15.04M		22%	20%	19%
DECEX	Decommissioning	C6	£3.5M		5%	5%	4%
Total			£67.92M	£75.43M			

6. Conclusion

A flexible, multi-fidelity cost model for floating offshore wind turbines, which can be implemented within any MDOA, has been developed. The model is flexible enough to be applied to different FOWT configurations, and the varying fidelity allows the cost and annual energy production to be calculated for a range of cases, from early design phases to more mature development stages. The work has been verified by comparing the present results against existing literature. The approach has been developed in a modular manner, making it suitable for other FOWT MDOA approaches. With cost being a huge driver within the floating offshore wind sector, implementing a flexible, multi-fidelity LCoE model for existing MDOA frameworks could help in identifying areas of higher cost, and to take into account a wider variety of costs than only CAPEX in early design. The optimization of the OC3 SPAR for a 5MW turbine, highlights it is possible to find alternative geometries in order to reduce the cost and inherently the LCoE, although further analyses (especially structural integrity checks) are necessary to confirm these results. The importance of the maximum allowable total angle of inclination, investigated through parametrically varying constraints, has been demonstrated, showing important cost reduction linked to the relaxation of this constraint. This does, however, have an impact on the power output, which is not considered within this paper. Overall, the findings of this work highlight the trade-off between the increased accuracy and the total time (not only the computational time, but the time necessary to gather the input information necessary) for the higher fidelity model, in comparison to the reduced time and accuracy for the lower fidelity model.

7. References

[1] RenewableUK, “Wind Energy Statistics.” https://www.energyvoice.com/renewables-energy-transition/wind/uk-wind/274960/uk-renewable-energy-capacity-double-2026/ (accessed Jan. 21, 2022).

[2] BBC-News, “World’s first floating wind farm starts generating electricity,” 2017. https://www.bbc.co.uk/news/uk-scotland-41652707#:~:text=The world’s first floating wind,officially opened by Nicola Sturgeon. (accessed Jun. 09, 2021).

[3] Y. Liu, S. Li, Q. Yi, and D. Chen, “Developments in semi-submersible floating foundations supporting wind turbines: A comprehensive review,” *Renew. Sustain. Energy Rev.*, vol. 60, pp. 433–449, 2016, doi: 10.1016/j.rser.2016.01.109.

[4] Matthew Hannon, Eva Topham, James Dixon, David Mcmillan, and Maurizio Collu, “Offshore wind, ready to float? Global and UK trends in the floating offshore wind market,” doi: 10.17868/69501.

[5] F. Dinmohammadi and M. Shafiee, “A fuzzy-FMEA risk assessment approach for offshore wind turbines,” *Int. J. Progn. Heal. Manag.*, vol. 31, no. 2, pp. 1–10, 2017, doi: 10.1002/bmc.3797.

[6] M. Lerch, M. De-Prada-Gil, C. Molins, and G. Benveniste, “Sensitivity analysis on the levelized cost of energy for floating offshore wind farms,” *Sustain. Energy Technol. Assessments*, vol. 30, no. March, pp. 77–90, 2018, doi: 10.1016/j.seta.2018.09.005.

[7] J. Rhodri and M. Costa Ros, “Floating Offshore Wind: Market and Technology Review,” 2015. doi: 10.1016/j.jcp.2016.01.012.

[8] C. Maienza, A. M. Avossa, F. Ricciardelli, D. Coiro, G. Troise, and C. T. Georgakis, "A life cycle cost model for floating offshore wind farms," *Appl. Energy*, vol. 266, no. October 2019, p. 114716, 2020, doi: 10.1016/j.apenergy.2020.114716.
[9] J. Dodd, "Devising O&M strategies for floating offshore," *Wind Power Monthly*, 2019. https://www.windpowermonthly.com/article/1585415/devising-o-m-strategies-floating-offshore (accessed Jun. 14, 2021).
[10] D. Fralie and C. Walsh, "Ports; a key enabler for the floating wind sector," 2020.
[11] L. Castro-Santos, E. Martins, and C. Guedes Soares, "Methodology to calculate the costs of a floating offshore renewable energy farm," *Energies*, vol. 9, no. 5, 2016, doi: 10.3390/en9050324.
[12] C. S. Laura and D. C. Vicente, "Life-cycle cost analysis of floating offshore wind farms," *Renew. Energy*, vol. 66, pp. 41–48, 2014, doi: 10.1016/j.renene.2013.12.002.
[13] A. Ghigo, L. Cottura, R. Caradonna, G. Bracco, and G. Mattiazzo, "Platform optimization and cost analysis in a floating offshore wind farm," *J. Mar. Sci. Eng.*, vol. 8, no. 11, pp. 1–26, 2020, doi: 10.3390/jmse8110835.
[14] S. Heidari, "Economic modelling of floating offshore wind power: Calculation of Levelized cost of energy," 2017.
[15] A. Ioannou, A. Angus, and F. Brennan, "Parametric CAPEX, OPEX, and LCOE expressions for offshore wind farms based on global deployment parameters," *Energy Sources, Part B Econ. Plan. Policy*, vol. 13, no. 5, pp. 281–290, 2018, doi: 10.1080/15567249.2018.1461150.
[16] C. Mone, T. Stehly, B. Maples, and E. Settle, "2014 Cost of Wind Energy Review," *Natl. Renew. Energy Lab.*, no. February, pp. 23–40, 2015.
[17] M. De Prada Gil, J. L. Domínguez-García, F. Díaz-González, M. Aragüés-Peñalba, and O. Gomis-Bellmunt, "Feasibility analysis of offshore wind power plants with DC collectiongrid," *Renew. Energy*, vol. 78, pp. 467–477, 2015, doi: 10.1016/j.renene.2015.01.042.
[18] C. Mone, T. Stehly, B. Maples, and E. Settle, "2019 Cost of Wind Energy Review," *Natl. Renew. Energy Lab.*, no. February, pp. 23–40, 2015.
[19] S. Alsubal, W. S. Alaloul, E. L. Shawn, M. S. Liew, P. Palaniappan, and M. A. Musarat, "Life Cycle Cost Assessment of Offshore Wind Farm: Kudat Malaysia Case," *Sustainability*, vol. 13, no. 14, p. 7943, 2021, doi: 10.3390/su13147943.
[20] L. Castro-Santos, D. Silva, A. R. Bento, N. Salvação, and C. Guedes Soares, "Economic feasibility of floating offshore wind farms in the North of Spain," *Ocean Eng.*, vol. 207, 2020, doi: 10.1016/j.oceaneng.2020.107393.
[21] A. Myhr, C. Bjerkseter, A. Ågotnes, and T. A. Nygaard, "Levelised cost of energy for offshore floating wind turbines in a lifecycle perspective," *Renew. Energy*, vol. 66, pp. 714–728, 2014, doi: 10.1016/j.renene.2014.01.017.
[22] J. M. Hegseth, E. E. Bachynski, and J. R. R. A. Martins, "Integrated design optimization of spar floating wind turbines," *Mar. Struct.*, vol. 72, no. March, p. 102771, 2020, doi: 10.1016/j.marstruc.2020.102771.
[23] M. Hall, B. Buckham, and C. Crawford, "Evolving offshore wind: A genetic algorithm-based support structure optimization framework for floating wind turbines," *Ocean. 2013 MTS/IEEE Bergen Challenges North. Dimens.*, 2013, doi: 10.1109/OCEANS-Bergen.2013.6608173.
[24] M. Hall, B. Buckham, and C. Crawford, "Hydrodynamics-based floating wind turbine support platform optimization: A basis function approach," *Renew. Energy*, vol. 66, pp. 559–569, 2014, doi: 10.1016/j.renene.2013.12.035.
[25] E. Wayman, "Coupled dynamics and economic analysis of floating wind turbine systems," *Dr. Diss. Massachusetts Inst. Technol.*, p. 146, 2006.
[26] N. Pollini, A. Pegalajar-Jurado, S. Dou, H. Bredmose, and M. Stolpe, "Gradient-based optimization of a 15 MW wind turbine spar floater," *J. Phys. Conf. Ser.*, vol. 2018, no. 1, 2021, doi: 10.1088/1742-6596/2018/1/012032.
[27] M. Leimeister, A. Kolios, and M. Collu, "Development of a Framework for Wind Turbine

Design and Optimization," *Modelling*, vol. 2, no. 1, pp. 105–128, 2021, doi: 10.3390/modelling2010006.
[28] I. Fylling and P. A. Berthelsen, "WINDOPT - An optimization tool for floating support structures for deep water wind turbines," *Proc. Int. Conf. Offshore Mech. Arct. Eng. - OMAE*, vol. 5, no. November, pp. 767–776, 2011, doi: 10.1115/OMAE2011-49985.
[29] A. C. Pillai, P. R. Thies, and L. Johanning, "Comparing frequency and time domain simulations for geometry optimization of a floating offshore wind turbine mooring system," *ASME 2018 1st Int. Offshore Wind Tech. Conf. IOWTC 2018*, pp. 1–11, 2018, doi: 10.1115/IOWTC2018-1006.
[30] S. Zhou, K. Müller, C. Li, Y. Xiao, and P. W. Cheng, "Global sensitivity study on the semisubmersible substructure of a floating wind turbine: Manufacturing cost, structural properties and hydrodynamics," *Ocean Eng.*, vol. 221, no. December 2020, p. 108585, 2021, doi: 10.1016/j.oceaneng.2021.108585.
[31] T. Gentils, L. Wang, and A. Kolios, "Integrated structural optimisation of offshore wind turbine support structures based on finite element analysis and genetic algorithm," *Appl. Energy*, vol. 199, pp. 187–204, 2017, doi: 10.1016/j.apenergy.2017.05.009.
[32] K. H. Chew, K. Tai, E. Y. K. Ng, and M. Muskulus, "Analytical gradient-based optimization of offshore wind turbine substructures under fatigue and extreme loads," *Mar. Struct.*, vol. 47, no. May, pp. 23–41, 2016, doi: 10.1016/j.marstruc.2016.03.002.
[33] L. E. S. Stieng and M. Muskulus, "Reliability-based design optimization of offshore wind turbine support structures using analytical sensitivities and factorized uncertainty modeling," *Wind Energy Sci.*, vol. 5, no. 1, pp. 171–198, 2020, doi: 10.5194/wes-5-171-2020.
[34] S. Dou, A. Pegalajar-Jurado, S. Wang, H. Bredmose, and M. Stolpe, "Optimization of floating wind turbine support structures using frequency-domain analysis and analytical gradients," *J. Phys. Conf. Ser.*, vol. 1618, no. 4, 2020, doi: 10.1088/1742-6596/1618/4/042028.
[35] P. Sclavounos, C. Tracy, and S. Lee, "Floating offshore wind turbines: Responses in a seastate Pareto optimal designs and economic assessment," *Proc. Int. Conf. Offshore Mech. Arct. Eng. - OMAE*, vol. 6, pp. 31–41, 2008, doi: 10.1115/OMAE2008-57056.
[36] A. Myhr and T. A. Nygaard, "Load reductions and optimizations on tension-leg-buoy offshore wind turbine platforms," *Proc. Int. Offshore Polar Eng. Conf.*, no. January, pp. 232–239, 2012.
[37] J. M. Hegseth, E. E. Bachynski, and B. J. Leira, "Effect of environmental modelling and inspection strategy on the optimal design of floating wind turbines," *Reliab. Eng. Syst. Saf.*, vol. 214, no. June 2020, p. 107706, 2021, doi: 10.1016/j.ress.2021.107706.
[38] J. Jonkman, S. Butterfield, W. Musial, and G. Scott, "Definition of a 5MW Reference Wind Turbine for Offshore System Development," *J. Offshore Mech. Arct. Eng.*, vol. 140, no. 3, 2018, doi: 10.1115/1.4038580.
[39] M. Mathiesen, A. K. Meyer, and B. Kvingendal, "Hywind Buchan Deep Metocean Design Basis RE2014-002," p. 129, 2014.
[40] J. N. Newman, *Marine hydrodynamics*. MIT press., 2018.
[41] M. Borg and M. Collu, "A comparison between the dynamics of horizontal and vertical axis offshore floating wind turbines," *Philos. Trans. R. Soc. A Math. Phys. Eng. Sci.*, vol. 373, no. 2035, 2015, doi: 10.1098/rsta.2014.0076.
[42] S. Hernández, *Optimum design of steel structures*, vol. 46, no. 1–3. 1998.
[43] L. Castro-Santos, A. Filgueira-Vizoso, I. Lamas-Galdo, and L. Carral-Couce, "Methodology to calculate the installation costs of offshore wind farms located in deep waters," *J. Clean. Prod.*, vol. 170, pp. 1124–1135, 2018, doi: 10.1016/j.jclepro.2017.09.219.
[44] M. Shafiee, F. Brennan, and I. A. Espinosa, "A parametric whole life cost model for offshore wind farms," *Int. J. Life Cycle Assess.*, vol. 21, no. 7, pp. 961–975, 2016, doi: 10.1007/s11367-016-1075-z.